THE EFFECTS OF CELL SIZE ON THE C:N:P OF PHYTOPLANKTON

BY

LIN POLLACK

A thesis submitted to the

Department of Biology

Mount Allison University

in partial fulfillment of the requirements for the

Bachelor of Science degree with Honours

April 24, 2021

TABLE OF CONTENTS

Acknowledgements

I would like to thank my supervisor, Dr. Justin Liefer, who has supported this study from start to finish. He's shown me that science can be both challenging and rewarding, and I am grateful to have completed this research in a lab that is inclusive and accessible through his efforts. I would also like to thank the Campbell and Waller labs for advice and equipment that helped maintain this research.

Without the enduring support of my friend Will, across the world, this thesis would not have been possible. I am also grateful to my housemates and my partner for their time. The four of you have formed my strategizing team for nearly a year. I hope your new and extensive phytoplankton knowledge serves all of you well in life.

I would like to give thanks to the Nova Scotia Power Fund for providing my ISRG funding over the summer, as well as NBIF and MTA for helping to fund this study.

List of Tables

List of Figures

ABSTRACT

Phytoplankton are the primary producers of the global ocean and their elemental stoichiometry (C:N:P) is a central feature of their ecology and biogeochemistry. Understanding the underlying mechanics of phytoplankton C:N:P variation is a key focus of marine biogeochemistry study. We used four diatom species of different sizes, *Thalassiosira pseudonana, Thalassiosira weissflogii, Odontella mobiliensis*, and *Stephanopyxis palmeriana*, to investigate how intracellular C:N:P varies with cell volume and determine the biochemical basis of that variation. To do this, we measured the main macromolecular components of C, N, and P in addition to the cellular quotas for these element in all four species during growth at near-optimal, nutrient replete conditions. This study found a negative relationship of C:P and N:P to cell volume that is supported by clear macromolecular mechanisms. This relationship is reflected by larger size-scaling exponents of P relative to C and N. As cell volume increased, species allocated relatively more N and P to residual pools and less to biosynthesis as represented by protein, RNA, and chl *a*. This study demonstrates that C:N:P variation and P-allocation across a size spectrum reflects a tradeoff between biosynthesis and storage.

INTRODUCTION

Phytoplankton regulate the global ocean

Marine phytoplankton are key regulators of global ocean processes, such as primary production that supports marine food webs (Yvon-Durocher et al. 2015, Winder and Sommer 2012) and the balance of CO_2 between the ocean and atmosphere that regulates Earth's climate (Follows and Dutkiewicz 2011, Winder and Sommer 2012, Diaz et al. 2008). All of these impacts are linked to the ways in which phytoplankton assimilate the key biological elements carbon (C), nitrogen (N), and phosphorus (P), with the stoichiometry of these elements (C:N:P) within phytoplankton cells being a key determinant of their ecosystem roles. Nutrient export to the deep ocean in particular is dependent upon the C:N:P of phytoplankton that are sinking from the ocean's surface; phytoplankton with a lower C:P and C:N, for example, export less carbon per each nutrient, which makes for less effective carbon burial (Galbraith and Martiny 2015). The C:N:P ratio also affects the efficiency of remineralization at depth by bacteria and archaea (Hessen et al. 2003). Phytoplankton C:N:P also affects the higher trophic levels, as it represents their food quality for consumers, and by extension the efficiency of consumer grazing (Hessen et al. 2003). There is a particular focus on how phytoplankton process phosphorous, as P is the ultimate limiting nutrient for growth and productivity in the global ocean (Bjorkman 2014, Falkowski 2000). The C:N:P of particular phytoplankton reflects their requirement and subsequently their uptake of C, N, and P, which affects resource competition in phytoplankton communities (Tilman 1982).

The C:N:P of phytoplankton regulates the C:N:P of dissolved nutrients in the ocean (Mouginot 2015), which was first suggested when Redfield noted that the C:N:P of surface phytoplankton closely resembled the C:N:P of dissolved nutrients at depth (Redfield 1958). The global C:N:P ratio of surface phytoplankton was defined by Alfred Redfield as 106:16:1 (Redfield 1958, Falkowski 2000, Quigg et al. 2003). The Redfield ratio is considered a cornerstone of ocean biogeochemistry (Falkowski 2000, Quigg et al. 2003) and was assumed to apply all regions of the ocean, but has been found to vary (Moreno and Martiny 2018) with consistent geographic patterns; for example, lower than Redfield proportions of C:P tend to occur in polar regions and oligotrophic gyres, and higher proportions are found in subtropical gyres (Moreno et al. 2018). C:N:P variances will affect all processes that the C:N:P ratio affects, so understanding why phytoplankton C:N:P

varies is important to understanding why and how it will change and how these processes will respond to global changes such as those brought on by climate change.

C:N:P Varies in Phytoplankton

Although several factors have been suggested as drivers of the variation in phytoplankton C:N:P observed across ocean regions, this variation is generally attributed to taxonomic differences in phytoplankton composition and the physiological responses of phytoplankton to growth conditions. (Moreno and Martiny, 2018). Multiple studies have noted significant differences in C:N:P at the species level (Zimmerman et al. 2013, Liefer et al. 2019) and have found phylogenetic links to cellular C:N:P (Garcia et al. 2018, Quigg et al. 2003) which may encompass differences in evolutionary history (Quigg et al. 2003), adaptive strategies to environmental conditions (Garcia et al. 2018) and in broad scope, to differences in cell size between eukaryotic phytoplankton and marine cyanobacteria (Bertilsson et al. 2003, Martiny et al. 2013). Regional variation has been linked to the phytoplankton species assemblage of the region (Martiny et al. 2013), as C:N:P varies across different phytoplankton taxa (Garcia et al. 2018, Quigg et al. 2003). Variation in the size of phytoplankton also affects their C:N:P (Garcia et al. 2018) and may correspond with global nutrient patterns (Moore et al. 2013, Moore and Brown 2020). Another potential driver of C:N:P variability is temperature, as phytoplankton N:P is found to be significantly lower at lower temperatures (Toseland 2013) and environmental conditions are linked to the global variation in phytoplankton species assemblages (Moore and Brown 2020).

Phytoplankton also exhibit high C:N:P plasticity in response to environmental factors such as temperature (Geider and LaRoche 2002, Yvon-Durocher et al. 2015, irradiance (Finkel et al. 2006, Geider and LaRoche 2002, Yvon-Durocher 2015), and nutrient conditions (Liefer et al. 2019). However, while this plasticity does affect C:N:P, differences in intracellular C:N:P between phytoplankton taxa are more significant (Geider and LaRoche 2002).

Macromolecular Composition

The C:N:P ratio of phytoplankton and its variation represents variation in the allocation of C, N, and P to macromolecules in the cell. Intracellular carbon is largely found in proteins, carbohydrates, and lipids (Finkel et al. 2016a, Zimmerman et al. 2014). The majority of cellular N is found in proteins (Lourenco et al. 2004), with smaller portions found in nucleic acids and, to a lesser extent, in chlorophylls (Geider and LaRoche 2002). Cellular P is often reported as being primarily allocated to nucleic acids (Geider and LaRoche 2002, Moreno and Martiny 2018), with the majority of P expected to be found in RNA, particularly ribosomal RNA, and a smaller fraction in DNA. However, storage pools of phosphorus have been shown to represent a majority of cellular allocation in some cases (Liefer et al. 2019) with polyphosphate being the most abundant form of P storage (Dyhrman, 2016). The extent to which cellular P is allocated to polyphosphate is poorly resolved as this has rarely been measured. Phospholipids are also an important P-containing macromolecule in the cell, but are a comparatively small proportion of the P quota (Geider & LaRoche 2002, Moreno and Martiny 2018). This macromolecular basis of phytoplankton C, N, and P allocation is known, although storage allocation remains a topic of discussion. A scarcity of macromolecular data inhibits our understanding of the systematic variation in C, N, and P allocation seen in phytoplankton, which has only recently been offered for the broadest taxonomic levels (Finkel et al. 2016b) and large cell size ranges (Finkel at al. 2016a).

C:N:P and Cell Size

Differences in basic cell structure and size of major phytoplankton taxa necessitates differences in the macromolecular composition of the cell, which is in turn reflected by differences in C:N:P. It can be difficult to separate the effects of phylogeny from the effects of cell size, as some taxa such as cyanobacteria and haptophytes contain generally small cells, while some taxa such as diatoms and dinoflagellates have a large size range with most cells larger than the other major taxa (Finkel et al. 2010). Differences in C:N:P between these major taxa reflect macromolecular differences due to their basic cell structure. Dinoflagellates generally have more carbohydrates than diatoms, which may be due to a thick carbohydrate- based cell wall in dinoflagellates rather than the silica- based cell wall characteristic of diatoms (Follows and Dutkiewiz 2011). Cyanobacteria tend to have a high protein content in comparison to other taxa

(Finkel et al. 2016b) which may be due to a higher protein requirement of their photosynthetic apparatus (Raven 1984). Cell size also affects phytoplankton function regardless of taxa, as it affects predation rate (Follows and Dutkiewiz 2011, growth rate (Finkel et al. 2016a, Follows and Dutkiewiz 2011), sinking rate (Finkel et al. 2016a, Follows and Dutkiewiz 2011) and nutrient storage (Finkel et al. 2016a), and may be linked to the macromolecular differences associated with these traits.

Cell size affects macromolecular composition through basic changes in cell structure and functional requirements. As cells increase in size, the surface area : volume ratio tends to decrease, so allocation to carbohydrates or phospholipids associated with the cell membrane may decrease with increasing size. This may cause variation in the effect of cell size on C:N:P across broad taxonomic ranges depending on the composition of the cell wall, as previously discussed with diatoms and dinoflagellates. Increased cell size also causes self-shading, increasing the chlorophyll content required for light harvest in proportion to other macromolecules (Finkel 2001).

The effects of cell size on macromolecular composition may be particularly relevant to diatoms, which have the largest variation in cell size of any major phytoplankton group (Finkel et al. 2010). A large central vacuole which takes up a great proportion of cell volume in larger diatoms (Sicko-Goad et al. 1984) and the aforementioned silicate cell wall in diatoms may increase the potential cell size effects. These two traits may contribute to a lower protein, carbohydrate, and lipid density, which doesn't increase with cell size to the same extent as other taxa, observed in diatoms (Finkel et al. 2016a). This creates intracellular space for other macromolecules and may provide for the larger allocation of P to storage, which would most likely be in the form of polyphosphate (Dhyrman 2016), observed in diatoms relative to other taxa (Liefer et al. 2019). This increased allocation of N and P to storage in diatoms, which increases with size, has been suggested as a driver of low C:P observed in polar regions and upwelling areas where large diatoms are a greater part of the phytoplankton community (Weber and Deutsch 2010, Moreno et al. 2018).

Cell size has also been found to affect growth rate (Mouginot et al. 2015), with a decrease in growth rate accompanying increasing cell size (Delong et al. 2010, Finkel et al. 2010, Follows and Dutkiewiz 2011). This in turn affects macromolecular composition. Higher growth rates require more biosynthetic machinery in the cell. Higher growth rates have therefore been hypothesized to result in a higher protein quota, as well as a higher RNA quota due to an increased

need for ribosomes (Moreno and Martiny 2018, Yvon-Durocher et al. 2015) which may be additionally affected by temperature due to the link between temperature and RNA function (Moreno and Martiny 2018). Consequently, an increasing cell size and correlating decrease in growth rate can be expected to reduce C:P, C:N, and N:P.

Study Design

This study will characterize the C:N:P ratio under replete conditions of four diatom species. Secondarily, the study will begin to address the effects of cell size on C:N:P variation with a breakdown of N and P into major N and P containing macromolecules to permit a better understanding of the underlying mechanisms of detected variation. Diatoms present a useful taxonomic group for this study because their large size range is advantageous to a study concerning cell size, and using one group of phytoplankton excludes the notable differences in growth rate and cell structure between different groups (Follows and Dutkiewicz 2011). Given the link between cell size and growth rate, and the link between growth rate and RNA content, we expect to find that the proportion of RNA decreases with increasing cell size. Additionally, we hypothesize that the proportion of P in storage macromolecules will increase with increasing cell size. This will be investigated using four species of diatom spanning a size range of four orders of magnitude, cultured at nutrient replete conditions at the same temperature in order to reduce environmental factors which could influence macromolecular composition beyond the effects of size.

METHODS

Culturing

Study Species

The four species studied were *Thalassiosira pseudonana* (CCMP 1335), *Thalassiosira weissflogii* (CCMP 1336), *Odontella mobiliensis* (CCMP 597), and *Stephanopyxis palmeriana* (CCMP 814), all of which were obtained from the National Center for Marine Algae and Microbiota (NCMA).

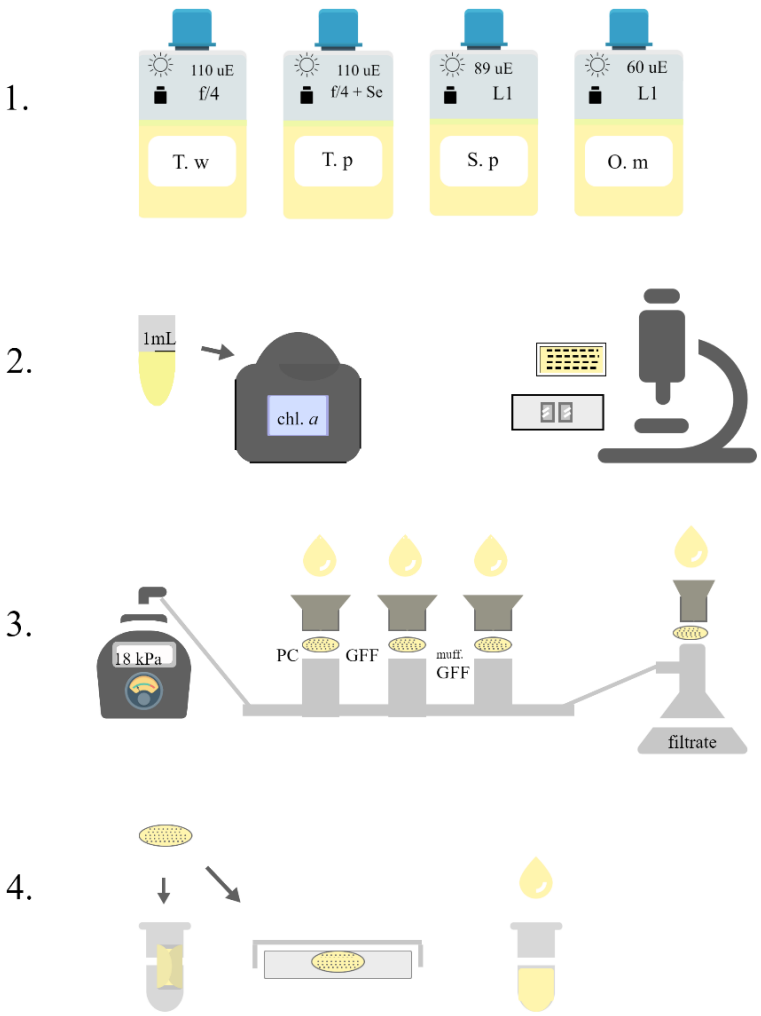

Figure 1. Culture and Sampling Methods Overview. Row **1** depicts, in descending order, the light conditions and media type used for each culture; all cultures were incubated at 18ºC. Row **2** depicts on the left a 1mL aliquot sample of live culture and the fluorometer used to measure in-vivo raw fluorescence. Row **2** depicts on the right a microscope with a Sedgewick rafter chamber used to count *T. weissflogii, S. palmeriana*, and *O. mobiliensis* samples and a hemocytometer used to count *T. pseudonana*. Row **3** depicts the filtration tower used for sampling. The filter pressure of 18kPa is listed as well as three filter types used and labels where filtrate was taken from an extension of the filter tower. Row **4** depicts filters folded and stored in tubes or petri slides, and aliquot sample stored in a tube.

Culture Conditions

All cultures were grown in triplicate at an ambient temperature of 18°C with a 12:12 light:dark cycle. *T. weissflogii* and *T. pseudonana* were cultured at a light intensity of 110µmol $m^{-2}s^{-1}$, *O. mobiliensis* at a light intensity of 60 µmol $m^{-2}s^{-1}$, and *S. palmeriana* at a light intensity of 89 µmol $m^{-2}s^{-1}$. Light levels were measured for each culture bottle in its designated location using a Walz ULM-500 light meter, and were reassessed when culture volume, vessel or location changed. Growth media was prepared with artificial seawater according to Berges et al. (2001). Artificial seawater was made using ultrapure (Milli-Q) water then filtered through a GF/F filter and a 0.2µm polycarbonate (PC) membrane filter, bottled, and autoclave-sterilized. *T. weissflogii* and *T. pseudonana* were cultured in f/4 media (Guillard 1975), and media for *T. pseudonana* was enriched with selenate at 50% of L1 media concentrations. *S. palmeriana* and *O. mobiliensis* were cultured in modified L1 media (Guillard and Hargraves 1993). Media was prepared in a sterile flow hood and nutrient stock solutions were filter-sterilized with 0.2µm PC membrane syringe filters prior to addition to media.

Culture Monitoring

1mL aliquot samples of *T.pseudonana, T. weissflogii*, and *O. mobiliensis* were taken during each cultures acclimation period and growth was tracked as chlorophyll *a* (chl *a*) in-vivo fluorescence using a Turner Trilogy Fluorometer. Growth was monitored daily prior to sampling for *T.pseudonana, T.weissflogii*, *and O.mobiliensis*. Due to its size, *S. palmeriana* was monitored via cell density every 2 days. Prior to filter-sampling, cell count samples were taken and evaluated for each species in addition to in-vivo fluorescence samples. All subsampling for the purposes of monitoring was performed in a sterile flow hood.

Cells density for *T. weissflogii*, *O. mobiliensis*, and *S. palmeriana* were measured in 1mL samples in a Sedgewick rafter chamber while cell density for *T. pseudonana* was measured in 12.5 µL samples settled onto a hemocytometer. All cell count samples were preserved immediately upon collection with 2% Lugol's solution. At high density, samples were diluted as needed. *T. weissflogii* cell counts obtained on the day of filter-sampling were stored at 7°C for four days prior

to counting; all other samples were counted on the day of collection. Monitoring counts were taken in duplicate or triplicate. Cell counts were taken in duplicate on sampling days when cultures were harvested.

Sampling

Filtration materials were acid-cleaned prior to use. Samples were collected onto filters at 18kPa vacuum pressure. Sampling took place in the middle of the light cycle for each culture. Samples for chl *a* were collected on 25mm Whatman glass fiber (GF/F) filters. Samples for particulate carbon and nitrogen (PCPN) and total particulate phosphorus (TPP) were collected on acid-rinsed combusted 25mm Whatman GF/F filters. These filters were prepared prior to sampling by soaking in 10% HCl for 48 hours, then rinsed 6-10 times with ultrapure water and dried while protected from dust. The dry filters were then combusted in a muffle oven at 450ºC for 3 hours. Samples for protein and RNA-DNA were collected on 25mm 0.8µm pore size polycarbonate filters. *O. mobiliensis* samples were rinsed with 0.2µm-filter sterilized artificial seawater (ASW) during filtration due to cells adhering to filter funnels. All other culture samples were rinsed with filter-sterilized ASW immediately after filtration of culture.

Samples for chl *a* were placed in 20mL scintillation vials and -80°C immediately after sampling. Samples for PCPN were placed on polycarbonate filter plates and stored at -20°C immediately after sampling then removed and stored in desiccator prior to analysis. Samples for TPP were collected onto filters and rinsed twice with 1mL 0.17M Na_2SO_4. Filters were stored in 20mL scintillation vials at -20°C. Prior to analysis, 2mL 0.017M MgSO4 was added to each sample, and samples dried in a drying oven at 60°C. Samples for protein and RNA-DNA were place in 2ml bead mile tube (MP Biomedicals, Lysing Matrix-D), flash frozen in liquid nitrogen, and stored at -80°C.

Elemental and Macromolecular Analyses

For PCPN analyses, dried filters were folded, packed tightly in tin capsules and analyzed by an Elementar PyroCube Combustion Elemental Analyzer using sulfanilamide as a reference standard.

Dried Samples for TPP were extracted using a protocol modified from Solorzano and Sharp 1980. Samples were combusted at 450°C for 6 hours. 5mL 0.2M HCl was added to each sample and vials were mixed, then placed at 90°C for 1 hour and mixed again. Sample was transferred to 1.7mL microtubes, centrifuged at 10,000x g for 5minutes, then transferred again to 1.7mL microtubes. Sample extracts were then transferred to a 96-well plate and analyzed for orothophosphate using a modification of the molybdenum blue method from Chen et al. 1956. The plate was mixed at 60 rpm for 5 minutes, then incubated at 37ºC for 1 hour protected from light.

For chl *a* analyses, samples were removed from the freezer and 5mL extraction solvent was added to each vial under dark conditions. The extraction solvent was a 3:2 solution of 90% acetone:DMSO (Shoaf and Lium 1976). Samples were then placed in the dark for 30 minutes, removed and mixed, then placed in the dark for 30 minutes. Each sample was mixed again, then subsamples were quickly transferred to cuvettes and chlorophyll *a* fluorescence was measured using a Turner Trilogy Fluorometer.

Samples for protein already in bead tubes were removed from -80ºC and extracted in 0.5mL of protein solubilization buffer (Brown and Audet 2008) and disrupted with a FastPrep-24 homogenizer at 6.5m/s for four 1-minute cycles, with cooling on ice for 1 minute after each round. Sample supernatant was then transferred to 1.7mL microtubes and centrifuged at 10,000x g for 5 minutes. 200uL supernatant was transferred and this extract was analyzed using the Pierce BCA Protein assay (Thermo Scientific), which is based on Lowry et al. 1951.

For RNA and DNA analyses, samples were extracted and analyzed according to Berdalet et al. 2005) and quantified by fluorescence in a opaque black 96-well plate.

All spectrophotometry and fluorometry performed in 96 well plates used a SpectraMax M3 plate reader (Molecular Devices).

Data Analyses

Correlations and Size Scaling

Correlations analyses were based on Pearson's correlation coefficient and calculated using Microsoft Excel. Size-scaling exponents were calculated for each elemental and macromolecular quota, assuming a power law function relates cell volume and cell density according to the following equation: $Q = a\ V^b$, where Q is the cellular quota of a given element or macromolecule in pg cell^{-1}, a is the y-intercept, V is cell volume in μm^3, and b is the scaling exponent.

To calculate size-scaling exponents, log-transformed cell volume and log-transformed cell quotas were compared with a simple Model I regression. The y-intercept of this regression corresponds to a and the linear slope corresponds to b, the size-scaling exponent. Regressions and 95% confidence intervals were calculated in Graph Pad Prism.

For size-scaling exponents to have predictive value, additional analyses would be needed to find fixed values for y-intercepts or different exponents should be calculated for different size ranges. Given the limited amount of data, size-scaling exponents were calculated with as a simple regression across all species without adjustments to the y-intercepts since scaling-exponents were only used for relative comparison across species in this study.

Size and growth rate

Biovolume was calculated using shape designations and formulae from Hillebrand et al. 1999. The size of each strain was calculated using the dimensions of 39 cells from each species. *O. mobiliensis* and *T. pseudonana* biovolumes were calculated using means of each dimension, due to limited cells visible in views necessary to obtain every dimension for every cell. Correspondingly, the standard deviation for these reported values is propagated from each mean dimension. All biovolumes are summarized in **Table 1.1** with standard deviation.

Mean growth rates were calculated from growth rates obtained in a period of 6-7 generations of growth prior to sampling and standard deviations were taken. Growth rates for *T. pseudonana, T. weissflogii*, and *O. mobiliensis* were taken from raw in-vivo fluorescence measurements and growth rates for *S. palmeriana* were taken from cell counts.

Replication

All cultures were grown and sampled in triplicate. An instrument error during particular carbon and particular nitrogen analysis prevented accurate analysis of one replicate culture of *T. pseudonana* and one replicate culture of *O. mobiliensis*. These replicates were excluded from data, and so *T. pseudonana* and *O. mobiliensis* were analyzed in duplicate while *T. weissflogii* and *S. palmeriana* were analyzed in triplicate.

C:N, N:P, C:P

C:N, N:P, and C:P were calculated as molar ratios from particulate carbon, particular nitrogen, and total particulate phosphorous data. These ratios were plotted against cell volume in **Figure 2.1**.

Macromolecular composition

To calculate the percentage of total N or P represented by each major macromolecule for each species, the macromolecule content was first multiplied by the expected N or P content of the macromolecule, based upon values reported in Geider and LaRoche 2002. A mean was taken of the replicate cultures, and this was compared to the total N or P content. These percentages are reported in **Table 2.1** and **Table 2.2.** A Pearson's Correlation test was run between cell volume and major macromolecules, and the R values from this test are reported in **Table 2.1** and **Table 2.2**.

Results

1. Size and Growth

The cell volumes of all four species were closely linked to their growth rates, which declined with increasing volume. The ratio of the cell sizes was 836 : 533 : 13 : 1. High variance for *S. palmeriana* is noted due to complications presented by its size and its propensity to form chains that lead to variance in cell counts. There is also about a 4.4fold different in growth rate, which decreases with increasing cell volume.

Strain	Biovolume (μm^3)	Growth Rate (d^{-1})
CCMP 1335 *T. pseudonana*	63.86 ± *20.00*	0.96 ± *0.20*
CCMP 1336 *T.weissflogii*	814.98 *s* ± *296.74*	0.72 ± *0.06*
CCMP 597 *O. mobiliensis*	34051.72 ± *14996.75*	0.27 ± *0.09*
CCMP 814 *S. palmeriana*	53380.97 ± *13585.58*	0.22 ± *0.20*

Table 1.1 Biovolume and growth rate measured for each cultured species and specifies strain. Error reported as standard deviation.

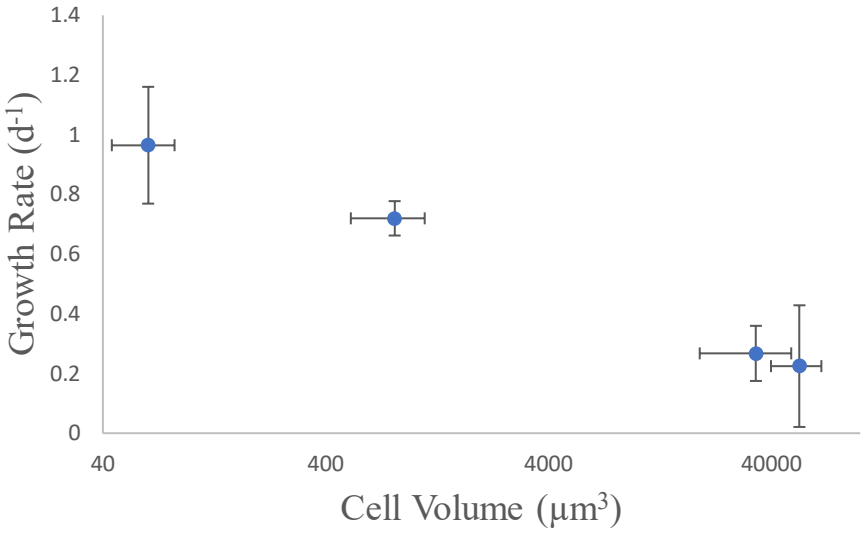

Figure 1.1 The relationship between the cell volumes of *T. pseudonana, T. weissflogii, O. mobiliensis*, and *S. palmeriana*, and their growth rates. Error bars indicate the standard deviations of the mean growth rate and mean cell volume for each species.

2. C:N:P Variation

The C:N, N:P, and C:P of each species had a negative relationship with cell size. The C:N, N:P, and C:P of *T. pseudonana* closely resembles Redfield proportions of 106:16:1, but all three ratios are markedly lower in *S. palmeriana* and showed a general decline with increasing cell size across the four species.

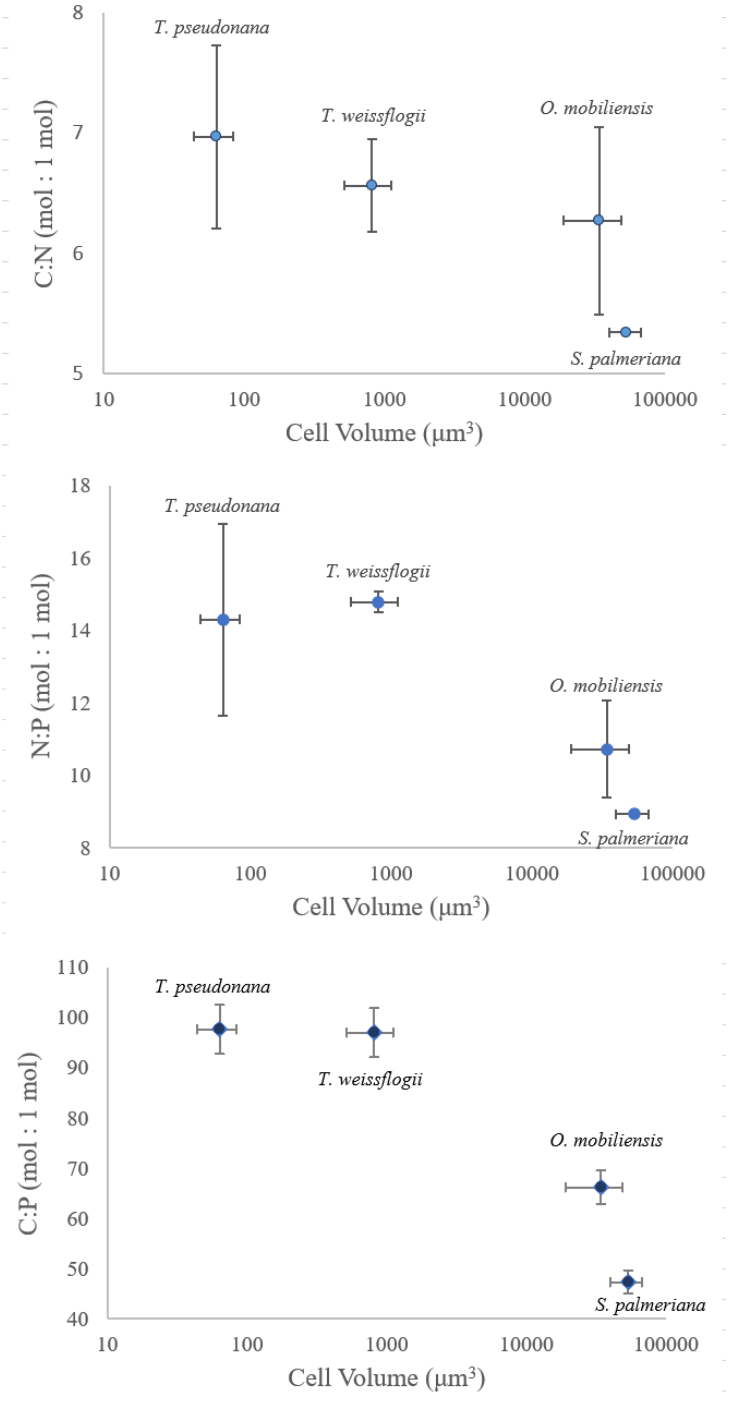

Figure 2.1 Relationship between a) C:N b) N:P, and c) C:P and the cell volumes of *T. pseudonana, T. weissflogii, O. mobiliensis*, and *S. palmeriana*.

Culture	C:N	N:P	C:P
T. pseudonana	6.97 ± *0.76*	14.31 ± *2.66*	97.70 ± *7.60*
T. weissflogii	6.57 ± *0.38*	14.79 ± *0.28*	97.03 ± *4.41*
O. mobiliensis	6.27 ± *0.78*	10.73 ± *1.33*	66.24 ± *0.05*
S. palmeriana	5.34 ± *0.52*	8.93 ± *0.76*	47.34 ± *0.76*

Table 2.1 Mean C, N, and P stoichiometry for all four species and their standard deviations.

3. Elemental Allocation to Macromolecules

N and P content of macromolecules was based upon values reported by Geider and LaRoche (2002). DNA and chlorophyll *a* account for a relatively small proportion of cellular P and N. In *T. pseudonana, T. weissflogii,* and *O. mobiliensis*, N is mostly found in proteins. In the largest diatom, *S. palmeriana,* residual N accounts for over half of intracellular N. Similarly, residual P significantly increases in proportion to other P-containing macromolecules with increasing cell volume. There is also a significant reduction in allocation of both P and N to RNA in the larger diatoms. Notably, the proportion of residual P in *O. mobiliensis* is smaller than the proportion of residual P in the smaller cell *T. weissflogii*. *O. mobiliensis* also has a larger proportion of P in DNA than the other three species.

	Protein	RNA	DNA	Chl. a	Residual
T. pseudonana	63.93	8.54	1.49	1.95	24.09
T. weissflogii	55.10	6.26	2.05	2.05	35.65
O. mobiliensis	45.72	6.09	0.81	0.81	43.02
S. palmeriana	42.74	3.97	1.09	1.09	51.18
Correlation to Cell Volume (R)	-0.78*	-0.81*			+0.78*

Table 3.1. Percent allocation of N to protein, RNA, DNA, chlorophyll a, and residual N for *T. pseudonana, T. weissflogii, O. mobiliensis*, and *S. palmeriana*. Proportion of N in proteins has a significant negative correlation with cell volume ($p = 0.007$), as does the proportion of N in RNA ($p = 0.004$). Proportion of residual N has a significant positive relationship with cell volume ($p = 0.007$).

	RNA	DNA	Residual
T. pseudonana	31.51	5.56	62.92
T. weissflogii	24.57	3.71	71.71
O. mobiliensis	17.20	12.5	70.30
S. palmeriana	9.31	2.45	88.25
Correlation to Cell Volume (R)	-0.96*	0.14	0.78*

Table 3.2. Percent allocation of P to RNA, DNA, and residual P for *T. pseudonana, T. weissflogii, O. mobiliensis,* and *S. palmeriana*. Proportion of P in RNA has a significant negative correlation with cell volume ($p < 0.001$). Proportion of residual P has a significant positive relationship with cell volume ($p = 0.008$). There is no significant correlation between proportion of P in DNA and cell volume.

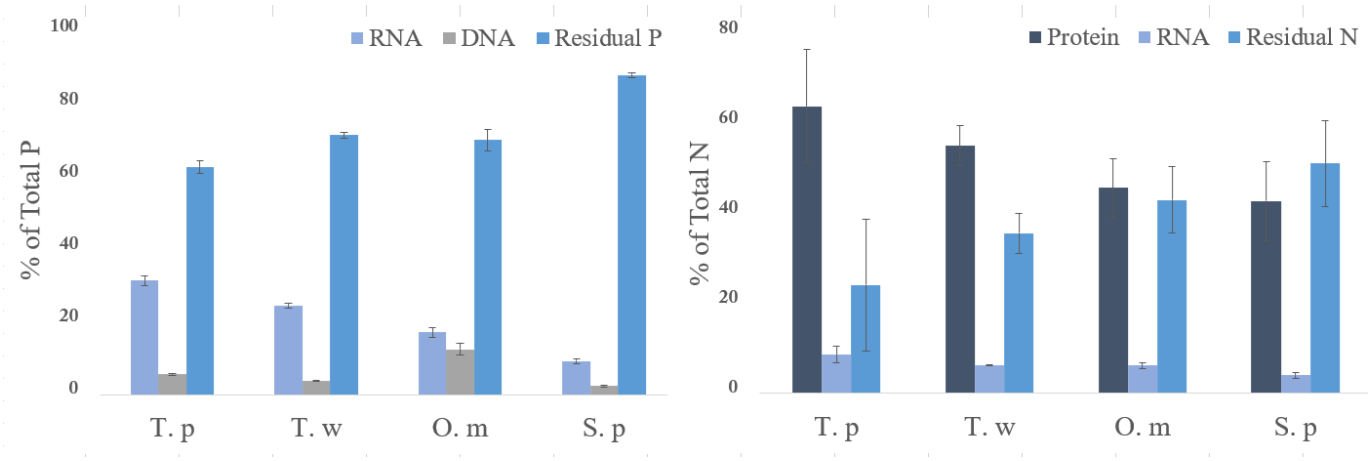

a. **b.**

Figure 3.1 N and P allocation within the cell as a percentage of total N and total P, with a depicting P-allocation and b depicting N-allocation. N and P content in each macromolecule based upon values in Geider and LaRoche (2002), and residual N and P reported as N and P content not accounted for by macromolecules studied. Species names are abbreviated to the following; T.p. as *T. pseudonana*, T.w. as *T. weissflogii*, O.m. as *O. mobilensis*, S.p. as *S. palmeriana*.

4. Size Scaling Of Element and Macromolecule Quota

Of the three elements, P has the highest size scaling far, and C has the lowest. Among macromolecules, Protein, RNA, DNA, and Chl. *a* have a lower size-scaling factor than residual N and P. These data have large confidence intervals due to the small number of points used for the calculation.

Element or Macromolecule	*b*	95% Confidence Interval
Carbon	0.748	(0.5667 , 0.9292)
Nitrogen	0.7813	(0.6073 , 0.9553)
Phosphorus	0.8591	(0.7213 , 0.9969)
Protein	0.723	(0.5464 , 0.8995)
Chl *a*	0.6556	(0.4571 , 0.8540)
RNA	0.702	(0.5403 , 0.8636)
DNA	0.8458	(0.6309 , 1.061)
Residual N	0.8911	(0.7554 , 1.027)
Residual P	0.8891	(0.6782 , 1.100)

Table 4.1. Size-scaling exponents (*b*) and confidence intervals of C, N, P, and measured macromolecules.

Discussion

C:N:P

Across the size range of the four species, the C:N, N:P, and C:P ratios decreased with increasing cell volume. This trend is shown in **Fig. 2.1,** and the elemental ratios are shown in **Table 2.1**. This trend contradicts a comprehensive study of phytoplankton C:N:P in nutrient replete cultures, which noted an increase in C:P and N:P with increasing cell size in diatoms (Garcia et al. 2018). One distinction between these studies is that the largest species we selected, *O. mobiliensis* and *S. palmeriana,* have substantially larger cell volumes than the diatoms species used in that study. This may indicate that the observed negative relationship between C:N:P and cell volume is visible on a broad size spectrum, but is less applicable on a smaller scale. This study also selected both pennate and centric diatoms and species that grew at different temperatures. Temperature adaptation can have a significant effect on C:N:P and intracellular nutrient allocation (Toseland 2013). Other C:N:P studies have noted lower mean C:P values across diatoms (Quigg et al. 2003), and have found the relationships between cell volume and C:P to more closely resemble the trend that we observed (Edwards et al. 2012, Parsons et al. 2019). These studies also noted a lower variance in C:N, which our data reflects with only a slight decrease in C:N as cell volume increases.

Storage Allocation

As predicted, allocation of intracellular N and P to residual pools increased with increasing cell size, depicted in **Table 3.1, Table 3.2,** and **Fig. 3.1**. We infer that Residual P represents P storage as other P-containing macromolecules, like phospholipids or metabolites such as ATP, have been shown to represent very small fractions of cellular P (Geider and LaRoche 2002; Liefer et al. 2019). This P storage likely represents orthophosphate (PO_4^{3-}) stored in intracellular vacuoles (Miyata et al. 1986) and predominantly the storage macromolecule polyphosphate, which can represent the largest portion of cellular P under certain conditions (Rhee 1973; Dyrhman 2016; Liefer et al. 2019). Residual N is expected to contain molecules which may serve as storage, such as dissolved nitrate and free amino acids (Moreno and Martiny 2018). *O. mobiliensis* may have been an exception to the observed trend in allocation to P storage, possibly due to the relatively

large proportion of P in its DNA. As depicted in **Table 3.2**, 12.5% of intracellular P in *O. mobiliensis* was found in DNA, compared to 3.7% in the smaller diatom *T. weissflogii*, which had a slightly higher proportion of residual P. Though a larger genome size is associated with larger cells, this relationship can be highly variable (Koester et al. 2010). There is also the possibility that *O. mobiliensis* had an unusually high DNA content during sampling due to entering sexual reproduction. However, spontaneous sexual reproduction in diatoms is rare and tends to affect a small portion of a population (Hedge et al. 2011) and no spermatogonium or auxospores (pre- and post- fertilization sexual stages) were observed in any sample cell counts taken during the monitoring or sampling periods of the study. Interestingly, the proportion of P in RNA for *O. mobiliensis* more closely fits the overall trend with cell volume, and this is reflected in a higher correlation of cell volume with RNA than of cell volume with residual P or DNA (**Table 3.1)**. This may indicate that with a higher steady requirement of P for DNA, allocation of P to RNA is made at the expense of P storage, which is a response that would favor maximized growth.

Biosynthetic Components

RNA and proteins are associated with biosynthesis, with the vast majority of RNA associated with rRNA in ribosomes (Sterner and Elser 2002). Thus, increased rRNA and proteins are expected with increased growth rate (Elser et al. 2000; Moreno and Martiny 2018, Zimmerman et al. 2014). Increasing proportions of residual N and P corresponded to decreasing proportions of N and P allocated to RNA (**Fig. 3.1)**. This suggests a tradeoff between allocation to nutrient storage and allocation to biosynthesis. Large size in diatoms is associated with lower growth rate, which was found in the four species studied (**Table 1.1**; **Fig. 1.1)**, suggesting a link between growth rate and macromolecular allocation that is difficult to distinguish from the effects of cell volume. However, diatoms have a uniquely large central vacuole (Sicko-Goad et al. 1984) which may allow them to reach a larger cell volume with a lower degree of size-scaling in their macromolecules (Finkel et al. 2016a). The silica cell wall characteristic of diatoms thickens with increasing cell volume (Brzezinski 1985) and doesn't require the additional macromolecular support necessary for other phytoplankton, which would increase carbohydrate, lipid, and protein requirements (Finkel et al. 2016a). This is why we hypothesized in this study that diatoms would increase N and P storage with increasing cell volume.

Tradeoffs between biosynthetic, structural, and storage macromolecules in diatoms, relative to other taxa, was supported for N by previous work that identified lower size-scaling exponents for protein (Finkel et al. 2016) and increased intracellular storage of dissolved inorganic nitrogen (Dortch et al. 1984) in diatoms. Similarly, we identified less allocation of N to protein (Table 3.1), and a lower size-scaling exponent for protein compared to cellular C and N (**Table 4.1)**. We also show similar support for a tradeoff with P, as the percentage of P allocated to RNA decreases with increasing cell volume and has the lowest size-scaling exponent among major macromolecules.

Implications

The changes in C:N:P across the four-species size range in this study suggest that cell volume on a broad scale is linked to cellular C:N:P through specific changes in the allocation of nutrients to macromolecules. Martiny et al. (2013) found that variation in C:N:P in the ocean could be linked to regional differences in dominant phytoplankton taxa, such as diatoms with low N:P and C:P vs. cyanobacteria with higher C:N:P (Martiny et al. 2013). This study suggests that differences in cell volume correlate to interspecific C:N:P and nutrient allocation differences. Cell size is currently used in some models to group phytoplankton traits (Follows and Dutkiewiz), and linkages demonstrated between cell volume and intracellular nutrient allocation positions cell volume as a potentially useful trait for predicting C:N:P across ocean regions. Moreno et al. (2018) demonstrated that the assumption of increased P storage with increased cell size enabled modelling to broadly predict global patterns in C:N:P variation. Further research should be conducted to resolve the distinctions between the effects of cell size and the effects of growth rate, and to investigate the role of DNA content in the nutrient allocation and C:N:P trends correlated with cell volume.

References

Andersen, R.A. 2005. Algal Culturing Techniques. Elsevier.

Berdalet, E., Roldán, C., Olivar, M., and Lysnes, K. 2005. Quantifying RNA and DNA in planktonic organisms with SYBR Green II and nucleases. Part A. Optimisation of the assay. Scientia Marina **69**. doi:10.3989/scimar.2005.69n11.

Berges, J.A., Franklin, D.J., and Harrison, P.J. 2001. Evolution of an artificial seawater medium: improvements in enriched seawater, artificial water over the last two decades. Journal of Phycology **37**(6): 1138–1145. doi:10.1046/j.1529-8817.2001.01052.x.

Björkman, K.M. 2014. Polyphosphate goes from pedestrian to prominent in the marine P-cycle. PNAS **111**(22): 7890–7891. National Academy of Sciences. doi:10.1073/pnas.1407195111.

Brown, C., MacKinnon, J., Cockshutt, A., Villareal, T., and Campbell, D. 2008. Flux capacities and acclimation costs in Trichodesmium from the Gulf of Mexico. Marine Biology **154**: 413–422. doi:10.1007/s00227-008-0933-z.

Brzezinski, M.A. 1985. The Si:C:N ration of marine diatoms: interspecific variability and the effect of some environmental variables. Journal of Phycology **21**(3): 347–357. doi:10.1111/j.0022-3646.1985.00347.x.

DeLong, J.P., Okie, J.G., Moses, M.E., Sibly, R.M., and Brown, J.H. 2010. Shifts in metabolic scaling, production, and efficiency across major evolutionary transitions of life. PNAS **107**(29): 12941–12945. National Academy of Sciences. doi:10.1073/pnas.1007783107.

Diaz, J., Ingall, E., Benitez-Nelson, C., Paterson, D., de Jonge, M.D., McNulty, I., and Brandes, J.A. 2008. Marine polyphosphate: a key player in geologic phosphorus sequestration. Science **320**(5876): 652–655. doi:10.1126/science.1151751.

Dortch, Q., Clayton, J.R., Thoresen, S.S., and Ahmed, S.I. 1984. Species differences in accumulation of nitrogen pools in phytoplankton. Marine Biology **81**(3): 237–250. doi:10.1007/BF00393218.

Dyhrman, S. 2016. Nutrients and Their Acquisition: Phosphorus Physiology in Microalgae. pp. 155–183. doi:10.1007/978-3-319-24945-2_8.

Falkowski, P.G. 2000. Rationalizing elemental ratios in unicellular algae. Journal of phycology **36**(1): 3–6. Wiley-Blackwell. doi:10.1046/j.1529-8817.2000.99161.x.

Finkel, Z.V., and Irwin, A.J. 2001. Light absorption by phytoplankton and the filter amplification correction: cell size and species effects. Journal of Experimental Marine Biology and Ecology **259**(1): 51–61. doi:10.1016/S0022-0981(01)00225-8.

Finkel, Z.V., Matheson, K.A., Regan, K.S., and Irwin, A.J. 2010. Genotypic and phenotypic variation in diatom silicification under paleo-oceanographic conditions. Geobiology **8**(5): 433–445. doi:https://doi.org/10.1111/j.1472-4669.2010.00250.x.

Finkel, Z.V., Follows, M.J., and Irwin, A.J. 2016a. Size-scaling of macromolecules and chemical energy content in the eukaryotic microalgae. Journal of Plankton Research **38**(5): 1151–1162. doi:10.1093/plankt/fbw057.

Finkel, Z.V., Follows, M.J., Liefer, J.D., Brown, C.M., Benner, I., and Irwin, A.J. 2016b. Phylogenetic Diversity in the Macromolecular Composition of Microalgae. PLOS ONE **11**(5): e0155977. Public Library of Science. doi:10.1371/journal.pone.0155977.

Follows, M.J., and Dutkiewicz, S. 2011. Modeling Diverse Communities of Marine Microbes. Annual Review of Marine Science **3**(1): 427–451. doi:10.1146/annurev-marine-120709-142848.

Galbraith, E.D., and Martiny, A.C. 2015. A simple nutrient-dependence mechanism for predicting the stoichiometry of marine ecosystems. Proc. Natl. Acad. Sci. U.S.A. **112**(27): 8199–8204. doi:10.1073/pnas.1423917112.

Garcia, N.S., Sexton, J., Riggins, T., Brown, J., Lomas, M.W., and Martiny, A.C. 2018. High Variability in Cellular Stoichiometry of Carbon, Nitrogen, and Phosphorus Within Classes of Marine Eukaryotic Phytoplankton Under Sufficient Nutrient Conditions. Front. Microbiol. **9**. Frontiers. doi:10.3389/fmicb.2018.00543.

Geider, R., and La Roche, J. 2002. Redfield revisited: variability of C:N:P in marine microalgae and its biochemical basis. European Journal of Phycology **37**(1): 1–17. Taylor & Francis. doi:10.1017/S0967026201003456.

Guillard, R.R.L. 1975. Culture of Phytoplankton for Feeding Marine Invertebrates. *In* Culture of Marine Invertebrate Animals: Proceedings — 1st Conference on Culture of Marine Invertebrate Animals Greenport. *Edited by* W.L. Smith and M.H. Chanley. Springer US, Boston, MA. pp. 29–60. doi:10.1007/978-1-4615-8714-9_3.

Guillard, R.R.L., and Hargraves, P.E. 1993. *Stichochrysis immobilis* is a diatom, not a chrysophyte. Phycologia **32**(3): 234–236. Taylor & Francis. doi:10.2216/i0031-8884-32-3-234.1.

Guillard, R.R.L., and Ryther, J.H. 1962. Studies of marine planktonic diatoms: I. *Cyclotella nana Hustedt*, and *Detonula confervacea* (Cleve) Gran. Can. J. Microbiol. **8**(2): 229–239. NRC Research Press. doi:10.1139/m62-029.

Hegde, S., Narale, D.D., and Anil, A.C. 2011. Sexual reproduction in Odontella regia (Schultze) Simonsen 1974 (Bacillariophyta). Current Science **101**(2): 222–225. Temporary Publisher.

Hillebrand, H., Dürselen, C.-D., Kirschtel, D., Pollingher, U., and Zohary, T. 1999. Biovolume Calculation for Pelagic and Benthic Microalgae. Journal of Phycology **35**(2): 403–424. doi:10.1046/j.1529-8817.1999.3520403.x.

Koester, J.A., Swalwell, J.E., von Dassow, P., and Armbrust, E.V. 2010. Genome size differentiates co-occurring populations of the planktonic diatom Ditylum brightwellii(Bacillariophyta). BMC Evol Biol **10**(1): 1. doi:10.1186/1471-2148-10-1.

Liefer, J.D., Garg, A., Fyfe, M.H., Irwin, A.J., Benner, I., Brown, C.M., Follows, M.J., Omta, A.W., and Finkel, Z.V. 2019. The Macromolecular Basis of Phytoplankton C:N:P Under Nitrogen Starvation. Frontiers in Microbiology **10**: 763. doi:10.3389/fmicb.2019.00763.

Litchman, E., and Klausmeier, C.A. 2008. Trait-Based Community Ecology of Phytoplankton. Annual Review of Ecology, Evolution, and Systematics **39**(1): 615–639. doi:10.1146/annurev.ecolsys.39.110707.173549.

Martiny, A.C., Pham, C.T.A., Primeau, F.W., Vrugt, J.A., Moore, J.K., Levin, S.A., and Lomas, M.W. 2013. Strong latitudinal patterns in the elemental ratios of marine plankton and organic matter. Nature Geoscience **6**(4): 279–283. doi:10.1038/ngeo1757.

Miyata, K., and Hattori, A. 1986. A simple fractionation method for determination of phosphorus components in phytoplankton: Application to natural populations of phytoplankton in summer surface waters of Tokyo Bay. Journal of the Oceanographical Society of Japan **42**(4): 255–265. doi:10.1007/BF02114524.

Moore, C.M., Mills, M.M., Arrigo, K.R., Berman-Frank, I., Bopp, L., Boyd, P.W., Galbraith, E.D., Geider, R.J., Guieu, C., Jaccard, S.L., Jickells, T.D., La Roche, J., Lenton, T.M., Mahowald, N.M., Marañón, E., Marinov, I., Moore, J.K., Nakatsuka, T., Oschlies, A., Saito, M.A., Thingstad, T.F., Tsuda, A., and Ulloa, O. 2013. Processes and patterns of oceanic nutrient limitation. Nature Geoscience **6**(9): 701–710. Nature Publishing Group. doi:10.1038/ngeo1765.

Moore, T.S., and Brown, C.W. 2020. Incorporating environmental data in abundance-based algorithms for deriving phytoplankton size classes in the Atlantic Ocean. Remote Sensing of Environment **240**: 111689. doi:10.1016/j.rse.2020.111689.

Moreno, A.R., and Martiny, A.C. 2018. Ecological Stoichiometry of Ocean Plankton. Annual Review of Marine Science **10**(1): 43–69. doi:10.1146/annurev-marine-121916-063126.

Mouginot, C., Zimmerman, A.E., Bonachela, J.A., Fredricks, H., Allison, S.D., Mooy, B.A.S.V., and Martiny, A.C. 2015. Resource allocation by the marine cyanobacterium Synechococcus WH8102 in response to different nutrient supply ratios. Limnology and Oceanography **60**(5): 1634–1641. doi:10.1002/lno.10123.

Quigg, A., Finkel, Z.V., Irwin, A.J., Rosenthal, Y., Ho, T.-Y., Reinfelder, J.R., Schofield, O., Morel, F.M.M., and Falkowski, P.G. 2003. The evolutionary inheritance of elemental stoichiometry in marine phytoplankton. Nature **425**(6955): 291–294. Nature Publishing Group. doi:10.1038/nature01953.

Raven, J.A. 1984. A Cost-Benefit Analysis of Photon Absorption by Photosynthetic Unicells. New Phytologist **98**(4): 593–625. doi:10.1111/j.1469-8137.1984.tb04152.x.

Rhee, G.-Y. 1973. A Continuous Culture Study of Phosphate Uptake, Growth Rate and Polyphosphate in Scenedesmus Sp.1. Journal of Phycology **9**(4): 495–506. doi:10.1111/j.1529-8817.1973.tb04126.x.

Shoaf, W.T., and Lium, B.W. 1976. Improved extraction of chlorophyll a and b from algae using dimethyl sulfoxide. Limnology and Oceanography **21**(6): 926–928. doi:10.4319/lo.1976.21.6.0926.

Sicko-Goad, L.M., Schelske, C.L., and Stoermer, E.F. 1984. Estimation of intracellular carbon and silica content of diatoms from natural assemblages using morphometric techniques. Limnology and Oceanography **29**(6): 1170–1178. doi:10.4319/lo.1984.29.6.1170.

Solórzano, L., and Sharp, J.H. 1980. Determination of total dissolved phosphorus and particulate phosphorus in natural waters1. Limnology and Oceanography **25**(4): 754–758. doi:10.4319/lo.1980.25.4.0754.

Weber, T., and Deutsch, C. 2010. Ocean nutrient ratios governed by plankton biogeography. Nature **467**(7315): 550–554. doi:10.1038/nature09403.

Winder, M., and Sommer, U. 2012. Phytoplankton response to a changing climate. Hydrobiologia **698**(1): 5–16. doi:10.1007/s10750-012-1149-2.

Yvon-Durocher, G., Dossena, M., Trimmer, M., Woodward, G., and Allen, A.P. 2015. Temperature and the biogeography of algal stoichiometry. Global Ecology and Biogeography **24**(5): 562–570. doi:10.1111/geb.12280.

Zimmerman, A.E., Allison, S.D., and Martiny, A.C. 2014. Phylogenetic constraints on elemental stoichiometry and resource allocation in heterotrophic marine bacteria. Environ. Microbiol. **16**(5): 1398–1410. doi:10.1111/1462-2920.12329.